Exploration of plastic-like phases in alkylurea systems. A thermal and X-ray study

Hashimoto, Masao
Tajima, Fukue
Eda, Kazuo
Yamamura, Kimiaki
Okazaki, Tadashi

(Citation)
Journal of Molecular Structure, 734(1-3):23-33

(Issue Date)
2005-01

(Resource Type)
journal article

(Version)
Accepted Manuscript

(URL)
https://hdl.handle.net/20.500.14094/90000970

Exploration of Plastic-like Phases in Alkylurea Systems. A Thermal and X-ray Study

Masao Hashimoto,[a] Fukue Tajima,[a] Kazuo Eda,[a] Kimiaki Yamamura[a] and Tadashi Okazaki[b]
[a] *Department of Chemistry, Faculty of Science, Kobe University, Rokkodai-cho1-1, Nada-ku, Kobe 657-8501, Japan*
[b]*Department of General Education, Kobe City College of Technology*
8-3 Gakuen-higashi-machi, Nishi-ku, Kobe 651-2194, Japan

Abstract

Many of alkylureas ($H_2NCONHC_nH_{2n+1}$, C_n-U) exhibited phase transitions and those found for $C_{4,\ 8}$-U had fairly large entropy of transition, indicating formation of quasi-plastic phases. X-ray structure determinations of $C_{2,\ 5–14}$-U revealed a characteristic common hydrogen bond network to result in the formation of two-dimensional, plate-like supramolecules having crossed arrangement of alkyl groups. The crystal structures of $C_{2,\ 5–14}$-U were found to be built by stacking the corresponding supramolecules along the *a* axis. The phase transitions of $C_{10,\ 13,\ 14}$-U and those of $C_{8,\ 12}$-U were found to accompany shifts of supramolecules along the crystal *c* axis and along both the *b* and *c* axes respectively. The transitions found for $C_4,\ _8$-U were proved to be of order-disorder type associated with the disordering of the alkyl groups. The transition of C_4-U was found to be associated with a drastic twist of the plane of the NCON moiety. The transition temperatures of C_4-U and C_8-U were depressed significantly by doping C_3-U and C_7-U, respectively, to form corresponding mixed crystals.

Keywords: Phase transition; Quasi-plastic phases; Supramolecule; Crystal Structure

Introduction

It is known that *n*-alkanes undergo phase transitions at a temperature just below the individual melting point and the transition entropy ($\Delta_{\mathrm{trs}}S$) amounts to ca.1/3 – 1/2 of the entropy of melting ($\Delta_{\mathrm{fus}}S$) [1]. In these transitions, reorientational motions of the molecule as a whole take place in the high-temperature phase [2-6]. These transitions are of order-disorder type and the high temperature phases have been referred to as rotator or plastic phase. Long chain alcohols are also known to exhibit plastic phases [7,8].

Several *cis*-unsaturated fatty acids, the molecular structures of which are non-linear in contrast to *n*-alkanes, are known to undergo phase transitions with large $\Delta_{\mathrm{trs}}S$. It has been known that (*Z*)-9-octadecenoic acid (oleic acid) and (*Z*)-13-docosenoic acid (erucic acid) exhibit order-disorder type transitions and the high temperature phases contain disorder of the alkyl group [9,10].

The order-disorder type transitions found for the fatty acids are not associated with thermal motions of the molecule as a whole, but with those of the alkyl groups. One may expect similar phenomena for the crystals of alkylureas ($H_2NCONHC_nH_{2n+1}$) where flexible alkyl groups are attached to rigid hydrogen bond (H-bond) networks. In fact, a phase transition with a fairly large $\Delta_{\mathrm{trs}}S/\Delta_{\mathrm{fus}}S$ ratio has been reported for octylurea [11].

In the present work, we carried out systematic thermal analyses on a series of alkylureas to find that several homologues showed transitions with $\Delta_{\mathrm{trs}}S/\Delta_{\mathrm{fus}}S$ ratios of ca.0.2–0.6. Moreover, phase transitions with the ratio of ca.0.03–0.13 were frequently found for many homologues. Then, we determined the crystal structures of these compounds at various temperatures to obtain information on the nature of the transition.

On the bases of the thermal and X-ray structural studies, the transition mechanisms will be discussed. The melting point (T_{fus}) *vs.* n relationship found for alkylureas will be also mentioned briefly.

Experimental

Materials

Alkylureas ($H_2NCONHC_nH_{2n+1}$, abbreviated as C_n-U according to the number of the carbon atoms in the alkyl group (n)) with n = 1, 3, 5–10 were provided by Dr. Y. Mido. Compounds $C_{4,11\text{-}14}$-U were prepared by the reported method [12]. Ethylurea (C_2-U) was obtained from commercial source (nacalai tesque). The single crystals of $C_{4\text{–}14}$-U were grown by evaporating the solvents of their solutions at room temperature. The solvents used were methanol (C_9-U), ethanol ($C_{5,\ 6,\ 8}$-U), acetone ($C_{7,\ 10,\ 12,\ 13}$-U) and acetonitrile ($C_{4,\ 11,\ 14}$-U). The single crystal of C_2-U was selected directly from the commercial compound. In order to obtain single crystals of the intermediate phase of C_4-U, which was stable in the range of 320–345 K, an ethanol solution of the compound was maintained at 343 K to evaporate the solvent.

Thermal analysis

A commercial equipment (Mac Science/Bruker DSC 3100S) was used for the thermal analyses. The temperature ranged from 150 K to the melting point of individual compound. The results of the thermal analyses are summarized in Table 1. The purity determined by a DSC method was better than 99 % for all the compounds. Phase transitions were found for $C_{3\text{–}5,\ 8,\ 10,\ 12\text{–}14}$-U. The phases of a compound will be referred to as I, II, or III in the order of decreasing temperature from the melting point.

Crystal structure analysis

A SMART 1000/CCD diffractometer (Bruker) was employed for the diffraction measurements using graphite monochromated Mo Kα radiations (λ =0.71073 Å). Data collections were carried out at several temperatures when needed. The lattice parameters of C_8-U and C_4-U were determined at many temperatures. The structures were solved by the direct method and refined by full-matrix least-squares calculations based on F_o^2 using SHELXL-97 [13]. Nonhydrogen atoms of each compound were included in the least-squares calculations with anisotropic displacement parameters. All of the hydrogen atoms of the $C_{2,\,4\text{–}14}$-U, except for the cases mentioned below, were included in the refinement with isotropic displacement parameters.

For the phase I of C_8-U, the displacements parameters of the terminal methyl carbon atom (C8) were found to be abnormally large suggesting a disorder. Then, the C8 atom was divided into two sites (C8T and C8S) corresponding approximately to the *trans* and the *skew* positions with respect to the C6-C7 bond in the -C6-C7-C8 segment. For these two carbon atoms, isotropic displacement parameters were applied and the relevant hydrogen atoms were omitted in the calculations of the structure refinement. The populations of the C8T and C8S were ca. 0.35 and ca. 0.65, respectively.

The crystal data and details of the structure refinements are given in Table 2-7 for 18 crystalline phases of 12 compounds.

Since the data for phase II of C_4-U are omitted from these tables owing to the low accuracy of the structure determination, they will be given below. The crystal data at 350 K: monoclinic, space group $P2_1/c$, a = 23.482(6), b = 20.819(6), c = 9.252(2) Å, β = 96.831(5) °. The asymmetric unit contains six molecules (Mol-1, 2, 3, 4, 5 and 6). Many of the carbon atoms of the butyl groups exhibited extremely large displacement parameters indicating conformational disorders of the moieties. The position of the molecule as a whole of Mol-5 was found to split into two sites as a result of disorder (Mol-5a and 5b), that of Mol-6 as well (Mol-6a and 6b). The structures of the urea moieties of Mol-1, 2, 3 and 4 were almost reasonable. The alkyl carbon atoms of Mol-1, 2, 3 and 4 were located approximately, while those of Mol-5 and 6 could not be found. The final $R1$ (Fo>2$\sigma(I)$), $wR2(F\text{o}^2)$ and S were ca.0.19, 0.51 and 0.74 respectively.

The details of the present crystal structure analyses except for the case of C_4-U (phase II) have been deposited in the Cambridge Crystal Data Center under the number CCDC 236790–236807.[1]

---

footnote: [1] CCDC 236790–236807 contain the supplementary crystallographic data for this paper. These data can be obtained free of charge via www.ccdc.cam.ac.uk/data_request/cif, by emailing data_request@ccdc.cam.ac.uk, or by contacting The Cambridge Crystallographic Data Centre, 12, Union Road, Cambridge CB2 1EZ, UK; fax: +44 1223 336033.

Results and Discussion

Thermodynamic behaviors of alkylureas

As can be seen from Table 1, the melting points (T_{fus}) of alkylures do not exhibit any systematic dependence on n in the range from n = 4 to19. This feature is in contrast to the systematic relationship between n and T_{fus} (melting point alternation) found for such compounds as n-alkanes, α,ω-alkenedithiols, α,ω-alkanedicarboxylic acids, α,ω-alkanediols and α,ω-alkanediamines. The melting point alternation has been interpreted by regular differences in the van der Waals interaction that depends on n [14-17]. Almost constant T_{fus} values of the alkylureas can be ascribed to a common N-H···O H-bond network, the structural parameters of which remain substantially constant regardless of n (see, below).

Many alkylureas undergo phase transitions in the temperature range investigated. It is interesting that the $\Delta_{\text{trs}}S/\Delta_{\text{fus}}S$ ratios found for $C_{4,\ 8}$-U are comparable to the values reported for "rotator phase" of *n*-alkanes and related compounds [1-6].

Crystal structures of alkylureas

All-*trans* conformation of the alkyl group is common in the crystals of C_4-U (phase III) and C_{5-14}-U except for the phase I of C_8-U. The molecules of the latter group are planar and the molecular geometries are quite similar to one another regardless of n.

In Fig.1, one can see the H-bond network in the phase I of C_{10}-U. The N2-H3···O1 H-bond (HB_d: D in the figure) with the N···O distance (L_{NO}) of 2.941(2) Å contributes to make a cetrosymmetric dimer. Other two H-bonds, N2-H2···O1 (HB_{C1}: P) with L_{NO} of 2.935(2) Å and N1-H1···O1 (HB_{C2},: Q) with L_{NO} of 3.062 (2) Å connect each of the two H_2NCONH- groups (urea moieties) of the dimer to neighboring one related by *c*-glide symmetry to result in a chain-like structure (urea-chain) running along the *c* direction. Since the planes of the adjacent urea moieties in a urea-chain make an angle (θ_u) of ca. 54 °, it is not a planar, but a twisted chain.

For the H-bond networks in the crystals of C_{5-14}-U, the values of L_{NO} of HB_d, HB_{c1} and HB_{c2} are in the ranges of 2.95 ± 0.01, 3.06 ± 0.02 and 2.93 ± 0.02 Å, respectively. The values of θ_u are within a region from 54.0 ° to 55.4 ° except for C_5-U (57.5 °). Thus, the H-bond network is common among these crystals regardless of the length of the alkyl group.

In the crystal of C_2-U, the molecule is not planar, the terminal methyl group being in approximate *skew* position with respect to the N1-C1 bond. The H-bond network is similar to that described above, although the value of θ_u is ca. 81 °.

The H-bond system in the phase III of C_4-U differs completely from those described above as illustrated in Fig. 2. The urea moieties form a planar urea-chain through the two N-H···O H-bonds, HB_{C1} and HB_{C2} (P and Q in the figure respectively). An infinite two-dimensional H-bond network is constructed by means of the third H-bond (HB_L, L) that connects the neighboring urea-chains. It is characteristic of the phase III of C_4-U that there is no dimer unit and that the alkyl groups take a parallel arrangement. The H-bond system in the phase II of C_4-U will be discussed later.

In Fig. 3, one can see that the crystal of C_{10}-U (phase I) consists of a supramolecular unit formed by the H-bond network. It has a plate-like structure extending infinitely along the *b* and *c* directions. The supramolecules are stacked along the *a* axis to result in the over-all crystal characterized by a layer structure parallel to the *bc* plane. The crossed arrangement of the alkyl groups in the supramolecule that can be seen in Fig. 3 (a) is caused by the characteristic twist of the urea-chain. This structure seems to be unusual, although similar arrangement of alkyl chains has been reported for aliphatic amides [18,19].

Two adjacent supramolecules of C_{10}-U in the phase I are related by a 2-fold screw axis to accomplish efficient packing according to the projection to hallow principle [20], since both sides of the supramolecule (lamella surfaces) have fairly deep grooves as shown in Fig.4 (b). The supramolecules found in the crystals of C_{5-14}-U bear strong structural resemblance to one another owing to the common H-bond network. The thickness of the supramolecule and the smoothness of lamella surface, however, vary depending on the individual length of the alkyl group.

The crystals of $C_{5\text{-}14}$-U with the space group of $P2_1/c$ are built by stacking the corresponding supramolecules along the *a* axis. The main structural difference among these crystals is the magnitude of the mutual shift of the two adjacent supramolecules along the *c* direction. The stacking pattern in the crystals with the space group of $C2/c$ will be discussed later.

Phase transitions of C_{10}-U, C_{13}-U and C_{14}-U

The II–I phase transition of C_{10}-U proceeds maintaining the space group ($P2_1/c$). The crystal structure of the phase II of C_{10}-U viewed along the *c* axis is substantially identical to that of the phase I shown in Fig.3 (a). The structure viewed along the *b* axis, however, shows clear difference between the two phases as shown in Fig.5, indicating that the II–I transition accompanies a mutual shift of the supramolecules along the *c* axis.

The III–II transition of C_{13}-U, as well as the III–II and the II–I transitions of C_{14}-U, take place without the change in the space group ($P2_1/c$) following the same mechanism as that of C_{10}-U.

Phase transitions of C_8-U and C_{12}-U

In the cases of the transitions found for C_8-U and C_{12}-U, the space group varies between $P2_1/c$ and $C2/c$. The latter one will be discussed first, because the crystal structures of the relevant two phases are simple without disorders.

As can be seen from Figs. 4(b) and 4(c), the lamella surface of the supramolecule of C_{12}-U is rather smooth compared to that of C_{10}-U. Thanks to the smoothness of the lamella surface, it is not necessarily impossible that two adjacent supramolecules of C_{12}-U are related by a 2-fold axis in the crystal with the space group of $C2/c$.

The II-I transition of C_{12}-U accompanies a mutual shift of the adjacent supramolecules along the *c* direction that is analogous to those mentioned above. In addition, a shift of supramolecules along the *b* axis also occurs as shown in Fig. 6. The shift along the *b* axis is considered to be possible owing to the smoothness of the lamella surface.

The molecular structures of C_8-U at 344 and 360 K are shown in Fig.7. It is evident that the C1-----C7 moiety of the octyl group persists to take the all-*trans* conformation even in the phase I, in spite of fairly vigorous thermal motions of the atoms suggested by their considerably large displacement parameters. But, the methyl group exhibits a conformational disorder in the phase I and hence the II–I transition is of order-disorder type similar to the transitions of the fatty acids [9,10].

As can be seen from Fig.8, the adjacent supramolecules shift simultaneously along the *c* and *b* directions in the transition process. With respect to this feature, the transition mechanism of C_8-U is analogous to that of C_{12}-U. The lamella surface of the supramolecule of C_8-U in the phase II is rather flat (Fig. 4 (a)), while it has shallow grooves in the phase I owing to the orientational disorder of the methyl group. Therefore, it seems reasonable that the phases I and II take the space groups of $P2_1/c$ and $C2/c$ respectively.

Besides the disorder of the methyl group, there is also a subtle structural difference between the supramolecules in the phases I and II as demonstrated by the abrupt change in the magnitude of θ_u (see, Fig.9 (a)). It should be noted that even in the phase II the structure of the supramolecule of C_8-U varies gradually depending on temperature as indicated by the θ_u vs. T curve.

The mean thermal expansion coefficients of a, b and c in the phase II ($143 < T/$ K < 343) are ca. 26, -9.9 and 5.9 x 10^{-5} K^{-1}, respectively (see, Fig. 9 (b)). The relatively small expansion of the c axis can be ascribed to the presence of the two H-bonds, HB_{C1} and HB_{C2}. It is interesting that the sign of the temperature dependence of the a axis is opposite to that of the b axis. This phenomenon is related almost quantitatively with the increase in θ_u that causes an expansion and a contraction of the a and b axes respectively. The discontinuous expansion of the b axis at the II–I transition point is likely to be ascribed to an enlargement of the terminal part of the alkyl group due to the disorder.

When a certain amount of C_7-U is doped to the crystal of C_8-U to form a mixed crystal, $(C_7\text{-U})_x(C8\text{-U})_{1-x}$, cavities are likely to appear in the vicinity of the methyl groups of C_8-U molecules. They are expected to lower the potential barrier hindering the occurrence of the conformational disorder. In fact, the II–I transition temperature of the mixed crystal was lower than that of pure C_8-U crystal by ca. 50 K when x = ca. 0.2.

Only a part of the transition entropy $\Delta_{trs}S$ can be ascribed to the conformational disorder of the methyl group. Most of $\Delta_{trs}S$ is considered to be due to the difference in the lattice frequency spectrum between the phases I and II.

Phase transition of C_4-U

Detailed discussion on the structure of the phase II of C_4-U is difficult because of the low accuracy of the structure determined. It could be concluded, however, that the supramolecule in the phase II took twisted H-bond chains similar to the common one found in many alkylureas. Thus, the III–II transition accompanies drastic twists of the molecular planes. This type of change in the arrangement of the alkyl groups due to phase transition has been reported for hexadecanamide [21]. It was also confirmed that the structures of the butyl groups of Mol-1, 2, 3 and 4 deviated markedly from the all-*trans* conformation.

The urea-chains formed by two N-H···O H-bonds in the phases III and II are running along the *a* and *c* axes respectively. Since *c*/2 of the phase II (4.626 Å) and *a* of the phase III (4.663 Å) are comparable, the geometry of the urea-chain appears to remain almost constant in the phases II and III. In contrast, the *b* axis of the phase III expands at the transition point by ca. 17 % (comparison between *b* (phase III) and *b*/3 (phase II)) and the *b* axis of the phase III expands gradually with increasing temperature by ca. 2.5 % in the temperature range of $203 < T/K < 303$. The behavior of the *b* axis is probably associated with the twist of the H-bond chain and the latter observation suggests a pre-transition phenomenon. The *c* axis of the phase III (25.863 Å) and the *a* axis of the phase II (23.482 Å) correspond to the thickness of the supramolecule in the respective phases. The decrease in the thickness at the III-II transition temperature is likely to be due to the conformational changes of the butyl groups.

The magnitude of $\Delta_{trs}S$ associated with the III–II transition is thought to be mainly ascribed to the conformational disorders suggested by the large displacements parameters found for the carbon atoms of the butyl groups in the phase II.

The occurrence of the III–II transition, which may be regarded a kind of interface melting [9], is expected to be facilitated in a mixed crystal, $(C_3\text{-U})_x(C4\text{-U})_{1-x}$. In fact the III–II transition temperature was depressed by about 10 K when x = ca. 0.1.

The phase II of C_4-U, as well as the phase I of C_8-U, is a quasi-plastic phases with respect to the magnitude of $\Delta_{trs}S$. These materials are interesting because of their possible use for storing energy *via* phase transitions as in the cases of plastic crystals [22]. The formation of suitable mixed crystals is applicable to realize desirable transition temperature. Moreover, the common two-dimensional H-bond network found for C_n-U is attractive because of possible occurrence of proton jump in these materials at higher temperatures.

Acknowledgement

Thanks are due to Dr. Y. Mido for his generous gifts of the samples. This work was supported in part by a Grant-in-Aid No. 15550119 from Japan Society for the Promotion of Science.

References

[1] Landordt-Bernstein Tabellen, 6 Aufl., Ⅱ Band, 4 Teil, Kalorische Zustandsgroessen, Springer-Verlag, 1961.

[2] Müller, Proc. R. Soc. London, Ser. A, 138 (1932) 514.

[3] G. Ungar, J. Phys. Chem., 87 (1983) 689.

[4] J. Doucet, I. Denicolo and A. Craievich, J. Chem. Phys., 75 (1983) 1523.

[5] T. Yamamoto, J. Chem. Phys., 89 (1988) 2356.

[6] E. B. Sirota, H. E. King, D. M. Singer and H. H. Shao, J. Chem. Phys., 98 (1993) 5809.

[7] E. B. Sirota and X. Z. Wu, J. Chem. Phys., 105 (1996) 7763.

[8] T. Yamamoto, K. Nozaki and T. Hara, J. Chem. Phys., 92 (1990) 631.

[9] M. Kobayashi, F. Kaneko, K. Sato and M. Suzuki, J. Phys. Chem., 90 (1986) 6371.

[10] F. Kaneko, K. Yamazaki, M. Kobayashi, Y. Kitagawa, Y. Matsuura, K. Sato and M. Suzuki, J. Phys. Chem. B, 100 (1996) 9138.

[11] D. Wells and C. J. Drummond, Langmuir, 15 (1999) 4713.

[12] T. L. Davis, K. C. Blanchard, J. Am. Chem. Soc., 51 (1929) 1790.

[13] G. M. Sherdrick, “SHELXL-97, Program for the Refinement of Crystal Structures”, University of Göttingen, Germany, 1997.

[14] R. Boese, H-C Weiss, D. Bläster, Angew. Chem., Int. Ed. 38 (1999) 988.

[15] V. R. Thalladi, R. Boese, H. C. Weiss, Angew. Chem., Int. Ed., 39 (2000) 918.

[16] V. R. Thalladi, R. Boese, H. C. Weiss, J. Am. Chem. Soc., 122 (2000) 1186.

[17] V. R. Thalladi, M. Nüsse, R. Boese, J. Am. Chem. Soc., 122 (2000) 9227.

[18] J. D. Turner and E. C. Lingafelter, Acta Cryst., 8 (1955) 551.

[19] T. Sakurai, J. Phys. Soc. Jpn., 10 (1955) 1040.

[20] Kitaigorodsky, “Molecular Crystals and Molecules”, Academic Press, New York and London, 1973, Chapter 1.

[21] T. Sakurai and M. Yabe, J. Phys. Soc. Jpn., 13 (1958) 5.

[22] D. F. R. Gilson, J. Chem. Educ., 69 (1992) 23. R. Strauss, S. Braun, S. Dou, H. Fuess and A. Weiss, Z. Naturforsch., 51 a (1996) 871 and references therein.

Figure captions

Fig. 1 A stereo view of the overall H-bond network in the phase I of C_{10}-U. Atoms of the alkyl group except for C1 are omitted. A part of the atom-labels are shown. The symbols P, Q and D put beside broken lines correspond to the H-bonds HB_{c1}, HB_{c2} and HB_d respectively.

Fig. 2 A stereo view of the overall H-bond network in the phase III of C_4-U. Symbols P, Q and L put beside broken lines correspond to the H-bonds HB_{c1} (2.982(2) Å), HB_{c2} (2.918(2) Å) and HB_L (3.022(2) Å), respectively.

Fig. 3 Crystal structure of C_{10}-U (phase I). (a) and (b) are projections onto the *ab* and *ac* planes respectively. The half of each figure corresponds to a supramolecule of C_{10}-U extending along the *b* and *c* axes. Broken lines indicate H-bonds. A pair of the + and - signs attached to an alkyl group indicates inclination of the group with respect to the ac plane (+ and -: up- and downward respectively).

Fig. 4 Structures of the halves of the supramolecules depicted by space-filling models of atoms for featuring lamella surfaces. (a), (b) and (c) for C_8-U, C_{10}-U and C_{12}-U respectively.

Fig. 5 Shift of the supramolecule of C_{10}-U along the *c* axis due to the II–I transition. The supramolecules (thin and bold ones for the phases I and II respectively) in the both phases are depicted in the same frame. The corresponding molecules of the phases are intentionally superimposed in the right half of the figure so as to emphasize the shift in the left half of the figure. A pair of the + and - signs attached to an alkyl group indicates inclination of the group with respect to the ac plane (+ and -: up- and downward respectively).

Fig. 6 Shift of the supramolecule of C_{12}-U along the *b* axis due to the II–I transition. The molecules depicted by thin and bold lines correspond to those in the phases I and II respectively. As to the details of the figure, see the caption of the figure 5.

Fig. 7 Molecular structures of C_8-U: (a) at 344 (phase II) and (b) at 360 K (phase I).

Fig. 8 Shifts of the supramolecule of C_8-U due to the II–I transition: (a) and (b) indicate the shifts along the *b* and *c* axes respectively. The molecules depicted by thin and bold lines correspond to those in the phases I and II respectively. As to the details of the figure, see the caption of the figures 5 and 6.

Fig. 9 (a) Temperature dependence of θ_u. (b) Temperature dependencies of L_R and V_R, $L_R = L(T)/L(143\text{ K})$ where $L(T)$ = the length of *a, b or c* axis at T, and $V_R = V(T)/V(143\text{ K})$, where $V(T)$ = unit cell volume at T. The value of L_R corresponding to the *a* axis of the phase I is calculated by using ½ *a*.

Table 1 Thermodynamic data of alkylureas (C_n-U) with n = 1–14 obtained by DSC experiments. fus: melting; trs1 and trs2: transitions 1 and 2 respectively

Compound	T_{fus}	$\Delta_{fus}H$	$\Delta_{fus}S$	T_{trs1}	$\Delta_{trs1}H$	$\Delta_{trs1}S$	T_{trs2}	$\Delta_{trs2}H$	$\Delta_{trs2}S$
	K	kJ mol^{-1}	J K^{-1} mol^{-1}	K	kJ mol^{-1}	J K^{-1} mol^{-1}	K	kJ mol^{-1}	J K^{-1} mol^{-1}
C_1-U	372.0	12.5	33.5	-	-	-	-	-	-
C_2-U	356.7	9.6	26.9	-	-	-	-	-	-
C_3-U	370.2	11.9	32.2	291.3	2.4	8.2	-	-	-
C_4-U	365.4	10.8	29.6	346.2	0.7	2.1	310.5	6.3	20.4
C_5-U	375.2	21.0	55.9	355.1	2.5	7.2	-	-	-
C_6-U	383.0	22.4	58.6	-	-	-	-	-	-
C_7-U	386.1	29.0	75.2	-	-	-	-	-	-
C_8-U	374.6	24.4	65.1	353.2	11.8	33.4	-	-	-
C_9-U	380.3	38.9	102.1	-	-	-	-	-	-
C_{10}-U	385.3	38.8	100.7	294.4	1.3	4.3	-	-	-
C_{11}-U	385.6	38.4	99.6	-	-	-	-	-	-
C_{12}-U	379.2	46.6	123.0	275.4	1.3	4.8	-	-	-
C_{13}-U	384.6	46.0	119.6	306.5	2.8	9.0	261.6	1.5	5.8
C_{14}-U	387.4	50.9	131.3	369.2	1.7	4.7	227.1	1.0	4.6

Table 2 Crystal data and details of experiments and refinements for C_2-U, C_4-U (phase Ⅲ), and C_5-U (phase Ⅱ)

	C_2-U	C_4-U (phaseⅢ)	C_5-U (phase Ⅱ)
Formula	$C_3H_8ON_2$	$C_5H_{12}ON_2$	$C_6H_{14}ON_2$
Molecular weight	88.11	116.17	130.19
X-ray radiation	Mo Kα	Mo Kα	Mo Kα
Wavelength (Å)	0.71073	0.71073	0.71073
Crystal system	monoclinic	monoclinic	monoclinic
Space group	$P2_1/c$	$P2_1/c$	$P2_1/c$
a (Å)	8.315(7)	4.663(2)	13.026(3)
b (Å)	7.046(6)	5.736 (2)	7.208(2)
c (Å)	9.099(8)	25.863(8)	9.277(2)
β(°)	107.48(2)	94.627(5)	110.861(3)
Cell volume (Å^3)	508.4(8)	689.5(4)	813.9(3)
Z	4	4	4
D_c (g cm^{-3})	1.151	1.119	1.062
μ(Mo-Kα) (mm^{-1})	0.087	0.079	0.073
F(000)	192	256	288
Temperature (K)	297	293	299
Crystal color	colorless	colorless	colorless
Crystal size (mm)	0.65 ×0.33 ×0.15	0.50×0.36×0.13	0.39×0.18×0.09
Theta range (°)	2.57-27.13	3.16-27.38	3.28-27.54
Index range	h -5 to 10	h -5 to 6	h -13 to 16
	k -8 to 8	k -7 to 6	k -9 to 6
	l -10 to 11	l -32 to 32	l -12 to 11
Reflections collected	2691	3708	4561
Reflections unique	1043	1396	1701
R_{int}	0.0640	0.0325	0.0432
Reflections (I>2σ(I))	490	1050	802
$R_1(F)$ (I>2σ(I))	0.0856	0.0489	0.0490
$wR_2(F^2)$ for all	0.2321	0.1412	0.1241
Number of parameters	76	121	138
Goodness- of- fit for all reflections (F^2)	0.942	0.988	0.829
Weighting scheme	$w^{-1} = [\sigma^2(F_o^2)$ $+(0.1377p)^2$ $+0.00p$, $p = (F_o^2 + 2F_c^2)/3$	$w^{-1} = [\sigma^2(F_o^2)$ $+(0.0786p)^2$ $+0.1031p$, $p = (F_o^2 + 2F_c^2)/3$	$w^{-1} = [\sigma^2(F_o^2)$ $+(0.0690p)^2$ $+0.00p$, $p = (F_o^2 +$
Max. shift/esd	0.000	0.000	0.000
$\rho_{\max}$(eÅ^{-3})	0.291	0.208	0.138
$\rho_{\min}$(eÅ^{-3})	-0.233	-0.161	-0.138
CCDC no.	236790	236791	236792

Table 3 Crystal data and details of experiments and refinements for C_6-U, C_7-U, and C_8-U (phase I)

	C_6-U	C_7-U	C_8-U (phase I)
Formula	$C_7H_{16}ON_2$	$C_8H_{18}ON_2$	$C_9H_{20}ON_2$
Molecular weight	144.22	158.24	172.27
X-ray radiation	Mo Kα	Mo Kα	Mo Kα
Wavelength (Å)	0.71073	0.71073	0.71073
Crystal system	monoclinic	monoclinic	monoclinic
Space group	$P2_1/c$	$P2_1/c$	$P2_1/c$
a (Å)	12.976(3)	14.407(4)	16.41(2)
b (Å)	7.430(2)	7.529(2)	7.558(9)
c (Å)	9.287(2)	9.318(2)	9.32(1)
β(°)	92.730(4)	102.426(4)	93.17(3)
Cell volume (Å^3)	894.4(3)	987.1(4)	1154(2)
Z	4	4	4
D_c (g cm^{-3})	1.071	1.065	0.992
μ(Mo-Kα) (mm^{-1})	0.073	0.071	0.065
F(000)	320	352	384
Temperature (K)	297	296	360
Crystal color	colorless	colorless	colorless
Crystal size (mm)	0.48×0.34×0.20	0.67×0.54×0.07	0. 53×0.41×0.28
Theta range (°)	3.14-27.31	2.90-27.43	2.49-27.20
Index range	h -15 to 15	h -18 to 13	h -11 to 15
	k -9 to 8	k -9 to 9	k -9 to 9
	l -11 to 11	l -11 to 11	l -11 to 5
Reflections collected	4932	5494	2754
Reflections unique	1805	2058	1734
R_{int}	0.0353	0.0779	0.0697
Reflections (I>2σ(I))	1057	971	561
$R_1(F)$ (I>2σ(I))	0.0529	0.0786	0.1206
$wR_2(F^2)$ for all	0.1424	0.2253	0.3131
Number of parameters	155	161	122
Goodness- of- fit for all reflections (F^2)	0.897	0.897	0.781
Weighting scheme	$w^{-1} = [\sigma^2(F_o^2) +(0.0930p)^2 +0.00p$, $p = (F_o^2 + 2F_c^2)/3$	$w^{-1} = [\sigma^2(F_o^2) +(0.1281p)^2 +0.00p$, $p = (F_o^2 + 2F_c^2)/3$	$w^{-1} = [\sigma^2(F_o^2) +(0.2000p)^2 +0.00p$, $p = (F_o^2 + 2F_c^2)/3$
Max. shift/esd	0.000	0.000	0.000
ρ_{max}(eÅ^{-3})	0.162	0.306	0.306
ρ_{min}(eÅ^{-3})	-0.238	-0.183	-0.203
CCDC no.	236793	236794	236795

Table 4 Crystal data and details of experiments and refinements for C_8-U(phase II), C_9-U, and C_{10}-U (phase I)

	C_8-U (phase Ⅱ)	C_9-U	C_{10}-U (phase Ⅰ)
Formula	$C_9H_{20}ON_2$	$C_{10}H_{22}ON_2$	$C_{11}H_{24}ON_2$
Molecular weight	172.27	186.30	200.32
X-ray radiation	Mo Kα	Mo Kα	Mo Kα
Wavelength (Å)	0.71073	0.71073	0.71073
Crystal system	monoclinic	monoclinic	monoclinic
Space group	$C2/c$	$P2_1/c$	$P2_1/c$
a (Å)	32.020(6)	17.774(4)	18.336(4)
b (Å)	7.412(2)	7.462(2)	7.538(2)
c (Å)	9.315(2)	9.264(2)	9.294(2)
β(°)	97.939(4)	103.726(4)	94.584(4)
Cell volume (Å^3)	2189.6(7)	1193.7(5)	1280.5(4)
Z	8	4	4
D_c (g cm^{-3})	1.045	1.037	1.039
μ(Mo-Kα) (mm^{-1})	0.069	0.067	0.067
F(000)	768	416	448
Temperature (K)	299	297	296
Crystal color	colorless	colorless	colorless
Crystal size (mm)	0.58×0.38×0.22	0.58×0.44×0.07	0.50×0.46×0.05
Theta range (°)	2.57-27.42	2.36-27.22	2.23-27.50
Index range	h -40 to 41	h -22 to 18	h -15 to 23
	k -8 to 9	k -8 to 9	k -9 to 9
	l -12 to 10	l -11 to 11	l -12 to 11
Reflections collected	6149	6431	7184
Reflections unique	2283	2447	2677
R_{int}	0.0324	0.0350	0.0473
Reflections (I>2σ(I))	1396	1372	1139
$R_1(F)$ (I>2σ(I))	0.0607	0.0566	0.0474
$wR_2(F^2)$ for all	0.1725	0.1549	0.1126
Number of parameters	189	206	223
Goodness- of- fit for all reflections (F^2)	0. 955	0.856	0.786
Weighting scheme	$w^{-1} = [\sigma^2(F_o^2) +(0.1106p)^2 +0.00p$, $p = (F_o^2 + 2F_c^2)/3$	$w^{-1} = [\sigma^2(F_o^2) +(0.1033p)^2 +0.00p$, $p = (F_o^2 + 2F_c^2)/3$	$w^{-1} = [\sigma^2(F_o^2) +(0.0535p)^2 +0.00p$, $p = (F_o^2 + 2F_c^2)/3$
Max. shift/esd	0.001	0.000	0.000
$\rho_{\max}$(eÅ^{-3})	0.228	0.227	0.141
$\rho_{\min}$(eÅ^{-3})	-0.211	-0.245	-0.126
CCDC no.	236796	236797	236798

Table 5 Crystal data and details of experiments and refinements for C_{10}-U (phase II), C_{11}-U, and C_{12}-U (phase I)

	C_{10}-U (phase Ⅱ)	C_{11}-U	C_{12}-U (phase Ⅰ)
Formula	$C_{11}H_{24}ON_2$	$C_{12}H_{26}ON_2$	$C_{13}H_{28}ON_2$
Molecular weight	200.32	214.35	228.37
X-ray radiation	Mo Kα	Mo Kα	Mo Kα
Wavelength (Å)	0.71073	0.71073	0.71073
Crystal system	monoclinic	monoclinic	monoclinic
Space group	$P2_1/c$	$P2_1/c$	$C2/c$
a (Å)	18.007(4)	19.617(3)	42.43(1)
b (Å)	7.528(2)	7.594(1)	7.598(2)
c (Å)	9.273(2)	9.339(2)	9.295(2)
β(°)	96.371(4)	97.540(3)	95.624(4)
Cell volume (Å^3)	1248.5(4)	1379.3(4)	2982.3(1)
Z	4	4	8
D_c (g cm^{-3})	1.066	1.032	1.017
μ(Mo-Kα) (mm^{-1})	0.068	0.066	0.064
F(000)	448	480	1024
Temperature (K)	233	273	293
Crystal color	colorless	colorless	colorless
Crystal size (mm)	0.50×0.46×0.05	0.83×0.46x0.15	0.64×0.45×0.04
Theta range (°)	2.28-27.46	2.09-27.18	1.93-27.18
Index range	h -22 to 18 k -9 to 9 l -10 to 11	h -24 to 22 k -9 to 9 l -11 to 10	h -51 to 51 k -9 to 9 l -11 to 9
Reflections collected	6992	7314	7775
Reflections unique	2600	2751	2994
R_{int}	0.0491	0.0346	0.0551
Reflections (I>2σ(I))	1186	1853	1392
$R_1(F)$ (I>2σ(I))	0.0517	0.0600	0.0563
$wR_2(F^2)$ for all	0.1425	0.1767	0.1392
Number of parameters	223	229	246
Goodness- of- fit for all reflections (F^2)	0.754	0.982	0.898
Weighting scheme	$w^{-1} = [\sigma^2(F_o^2)$ $+(0.0878p)^2$ $+0.00p$, $p = (F_o^2 + 2F_c^2)/3$	$w^{-1} = [\sigma^2(F_o^2)$ $+(0.1150p)^2$ $+0.00p$, $p = (F_o^2 + 2F_c^2)/3$	$w^{-1} = [\sigma^2(F_o^2)$ $+(0.0634p)^2$ $+0.00p$, $p = (F_o^2 + 2F_c^2)/3$
Max. shift/esd	0.000	0.000	0.000
ρ_{max}(eÅ^{-3})	0.169	0.266	0.141
ρ_{min}(eÅ^{-3})	-0.228	-0.219	-0.142
CCDC no.	236799	236800	236801

Table 6 Crystal data and details of experiments and refinements for C_{12}-U (phase II), C_{13}-U (phase I), and C_{13}-U (phase II)

	C_{12}-U (phase Ⅱ)	C_{13}-U (phase Ⅰ)	C_{13}-U (phase Ⅱ)
Formula	$C_{13}H_{28}ON_2$	$C_{14}H_{30}ON_2$	$C_{14}H_{30}ON_2$
Molecular weight	228.37	242.4	242.4
X-ray radiation	Mo Kα	Mo Kα	Mo Kα
Wavelength (Å)	0.71073	0.71073	0.71073
Crystal system	monoclinic	monoclinic	monoclinic
Space group	$P2_1/c$	$P2_1/c$	$P2_1/c$
a (Å)	21.100(9)	23.124(8)	22.936(5)
b (Å)	7.364(3)	7.542(2)	7.413(2)
c (Å)	9.200(4)	9.299(3)	9.314(2)
β(°)	95.085(8)	99.751(7)	99.290(4)
Cell volume (Å^3)	1424(1)	1598.3(9)	1562.8(6)
Z	4	4	4
D_c (g cm^{-3})	1.065	1.007	1.030
μ(Mo-Kα) (mm^{-1})	0.067	0.063	0.064
F(000)	512	544	544
Temperature (K)	170	314	298
Crystal color	colorless	colorless	colorless
Crystal size (mm)	0.64×0.45×0.04	0.64×0.58×0.09	0.64×0.58×0.09
Theta range (°)	2.91-27.47	2.68-27.56	1.80-27.55
Index range	h -16 to 26	h -23 to 29	h -26 to 28
	k -9 to 9	k -8 to 9	k -8 to 9
	l -11 to 11	l -11 to 11	l -11 to 11
Reflections collected	7411	8813	8569
Reflections unique	2916	3318	3232
R_{int}	0.0930	0.0862	0.0667
Reflections ($I>2\sigma(I)$)	1331	987	1552
$R_1(F)$ ($I>2\sigma(I)$)	0.0793	0.0690	0.0729
$wR_2(F^2)$ for all	0.2223	0.2057	0.1827
Number of parameters	257	247	274
Goodness- of- fit for all reflections (F^2)	0.845	0.795	0.883
Weighting scheme	$w^{-1} = [\sigma^2(F_o^2)$ $+(0.1205p)^2$ $+0.00p$, $p = (F_o^2 + 2F_c^2)/3$	$w^{-1} = [\sigma^2(F_o^2)$ $+(0.1157p)^2$ $+0.00p$, $p = (F_o^2 + 2F_c^2)/3$	$w^{-1} = [\sigma^2(F_o^2)$ $+(0.0965p)^2$ $+0.00p$, $p = (F_o^2 + 2F_c^2)/3$
Max. shift/esd	0.000	0.000	0.000
ρ_{max}(eÅ^{-3})	0.348	0.194	0.231
ρ_{min}(eÅ^{-3})	-0.348	-0.177	-0.226
CCDC no.	236802	236803	236804

Table 7 Crystal data and details of experiments and refinements for C_{13}-U (phase III), C_{14}-U (phase II), and C_{14}-U (phase III)

	C_{13}-U (phaseⅢ)	C_{14}-U (phaseⅡ)	C_{14}-U (phaseⅢ)
Formula	$C_{14}H_{30}ON_2$	$C_{15}H_{32}ON_2$	$C_{15}H_{32}ON_2$
Molecular weight	242.4	256.43	256.43
X-ray radiation	Mo Kα	Mo Kα	Mo Kα
Wavelength (Å)	0.71073	0.71073	0.71073
Crystal system	monoclinic	monoclinic	monoclinic
Space group	$P2_1/c$	$P2_1/c$	$P2_1/c$
a (Å)	21.99(1)	23.601(7)	23.257(6)
b (Å)	7.405(3)	7.639(2)	7.472(2)
c (Å)	9.313(4)	9.326(3)	9.269(2)
β(°)	93.909(8)	94.882(6)	90.332(5)
Cell volume (Å^3)	1513(1)	1675.4(9)	1610.8(7)
Z	4	4	4
D_c (g cm^{-3})	1.064	1.017	1.057
μ(Mo-Kα) (mm^{-1})	0.066	0.063	0.066
F(000)	544	576	576
Temperature (K)	200	303	153
Crystal color	colorless	colorless	colorless
Crystal size (mm)	0.64×0.58×0.09	0.77×0.41×0.02	0.77×0.41×0.02
Theta range (°)	1.86-27.42	1.73-27.43	2.63-27.23
Index range	h -26 to 28	h -28 to 26	h -29 to 28
	k -9 to 8	k -8 to 9	k -6 to 9
	l -11 to 10	l -11 to 11	l -11 to 11
Reflections collected	7795	9234	8633
Reflections unique	3054	3445	3296
R_{int}	0.0594	0.0616	0.0648
Reflections (I>2σ(I))	1719	1359	1781
R_1(F) (I>2σ(I))	0.0801	0.0583	0.0602
wR_2(F^2) for all	0.2288	0.1660	0.1587
Number of parameters	274	280	291
Goodness- of- fit for all reflections (F^2)	0.937	0.810	0.882
Weighting scheme	$w^{-1} = [\sigma^2(F_o^2)$ $+(0.1032p)^2$ $+1.6681p$, $p = (F_o^2 + 2F_c^2)/3$	$w^{-1} = [\sigma^2(F_o^2)$ $+(0.0730p)^2$ $+0.00p$, $p = (F_o^2 + 2F_c^2)/3$	$w^{-1} = [\sigma^2(F_o^2)$ $+(0.0875p)^2$ $+0.00p$, $p = (F_o^2 + 2F_c^2)/3$
Max. shift/esd	0.000	0.000	0.000
ρ_{max}(eÅ^{-3})	0.298	0.177	0.227
ρ_{min}(eÅ^{-3})	-0.239	-0.169	-0.175
CCDC no.	236805	236806	236807

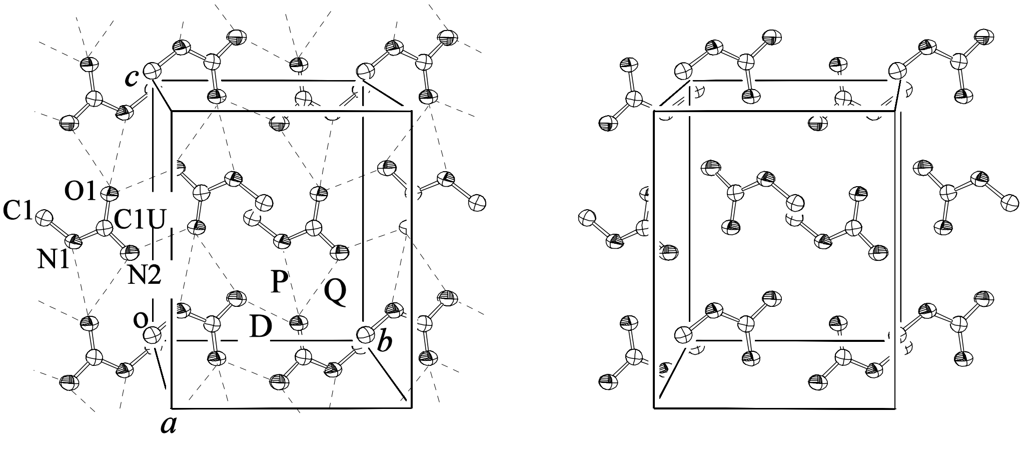

Fig. 1 by Hashimoto et al.

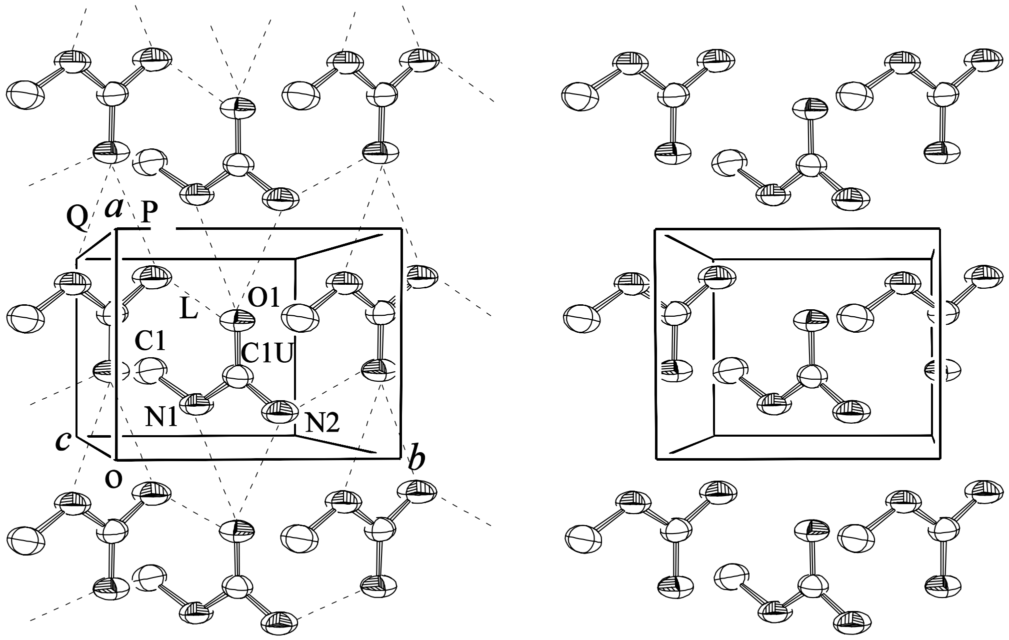

Fig. 2 by Hashimoto et al.

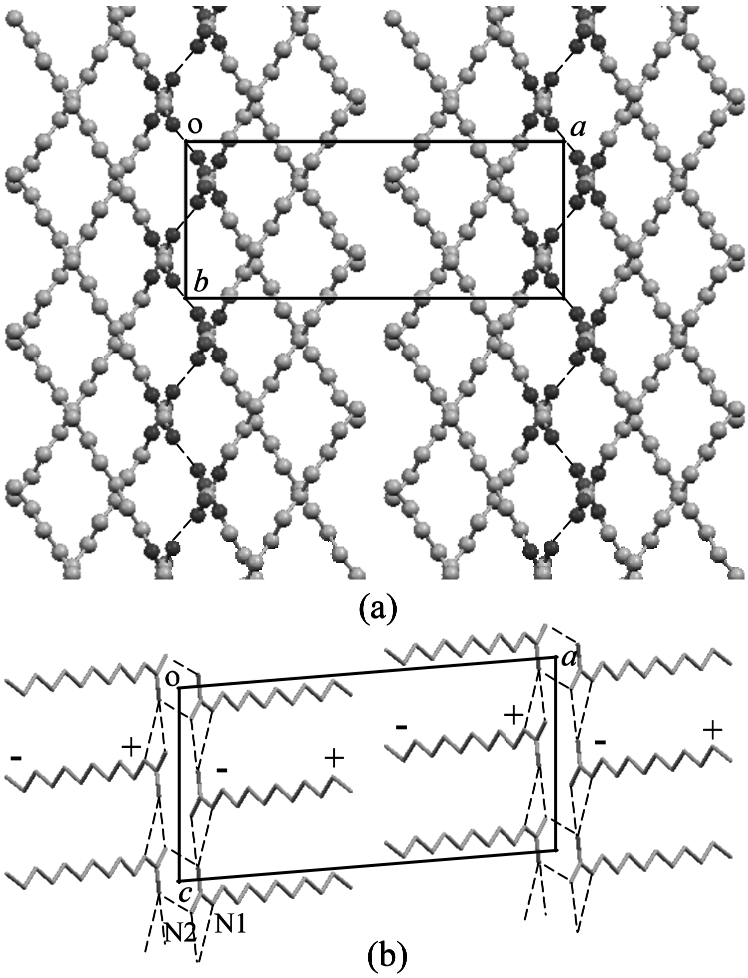

(a)

(b)

Fig. 3 by Hashimoto et al.

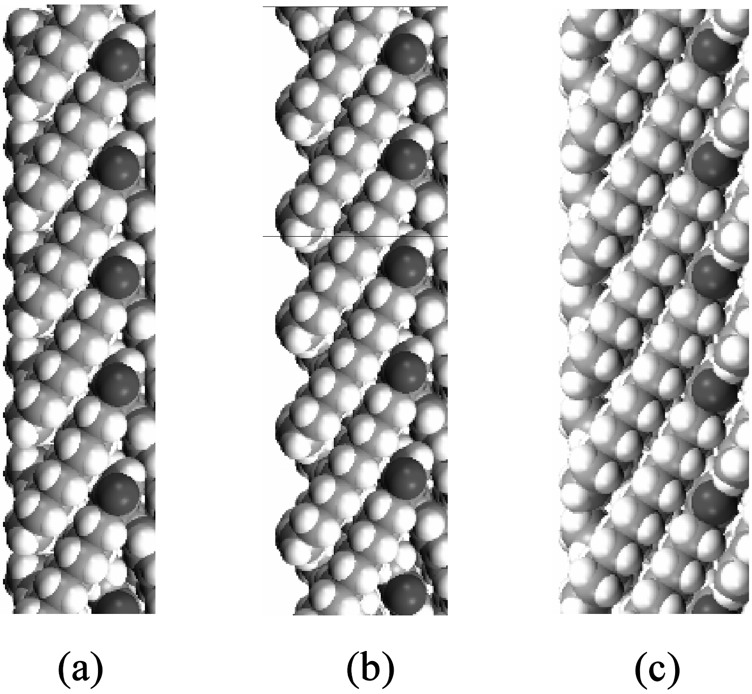
(a) (b) (c)

Fig. 4 by Hashimoto et al.

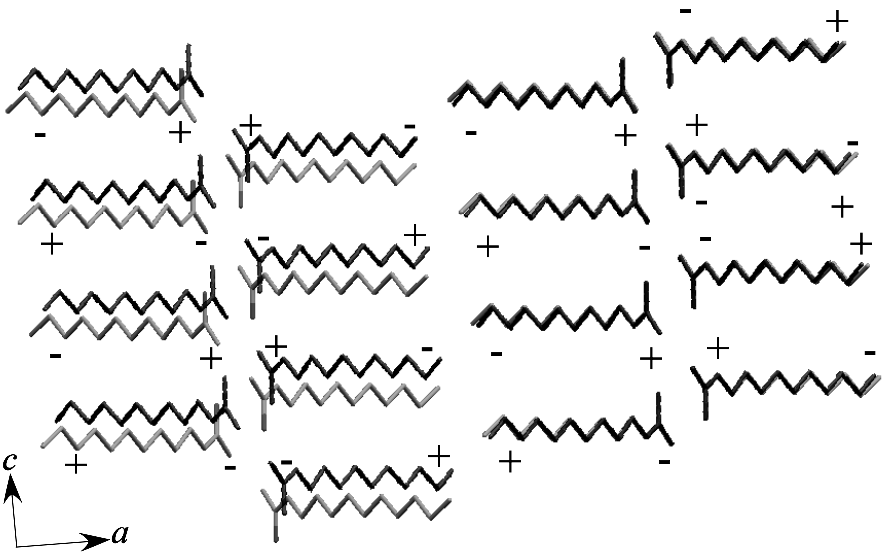

Fig. 5 by Hashimoto et al.

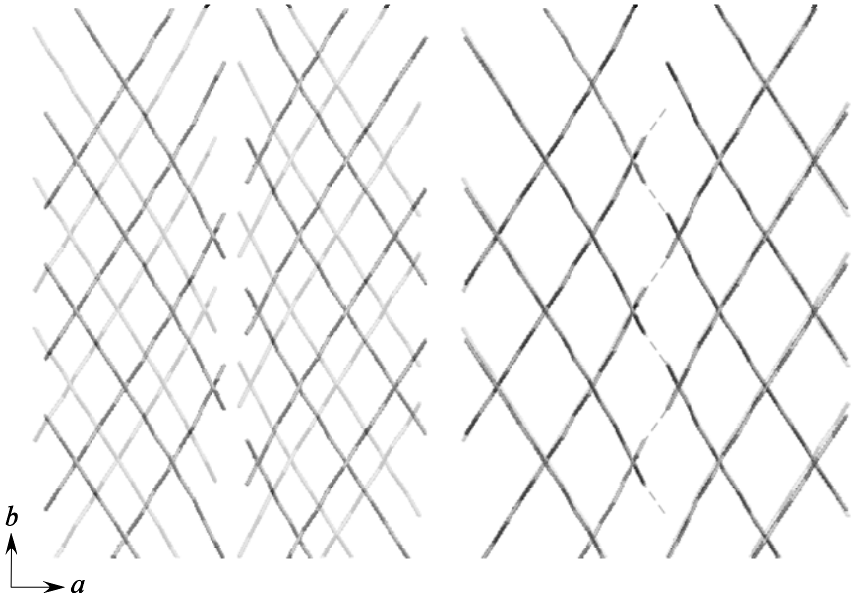

Fig. 6 by Hashimoto et al.

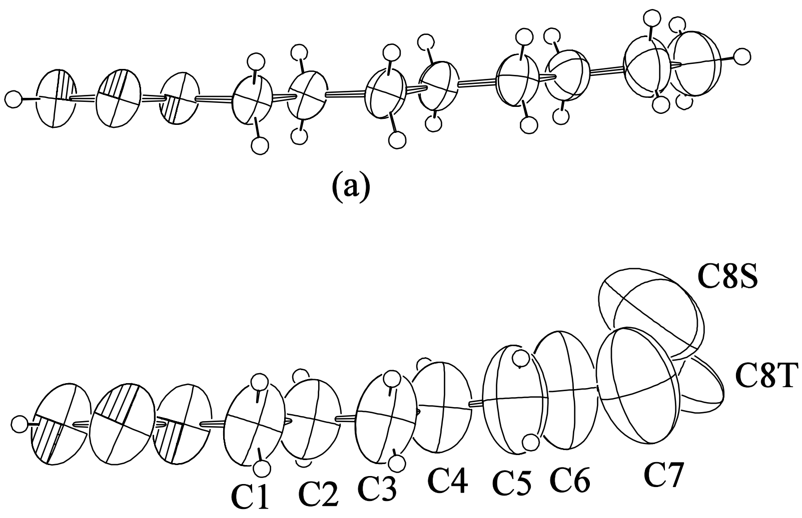

(a)

(b)

Fig. 7 by Hashimoto et al.

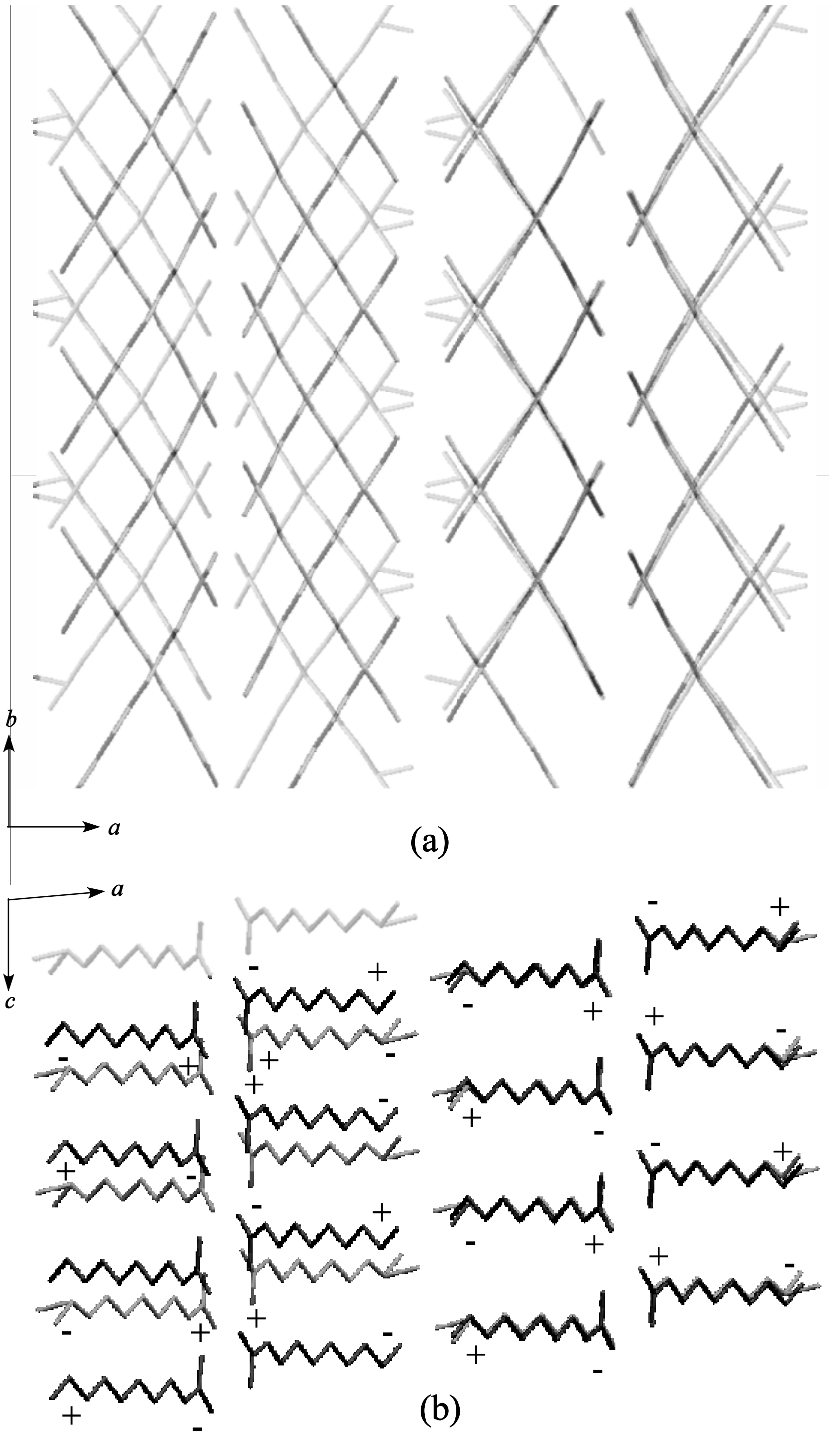

Fig. 8 by Hashimoto et al.

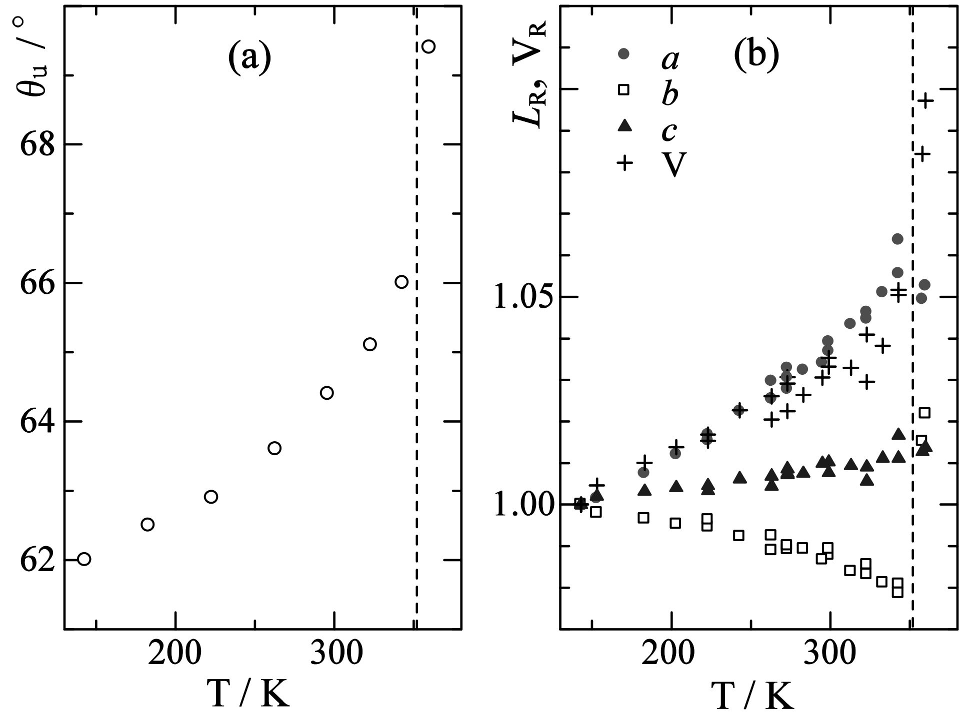

Fig. 9 by Hashimoto et al.